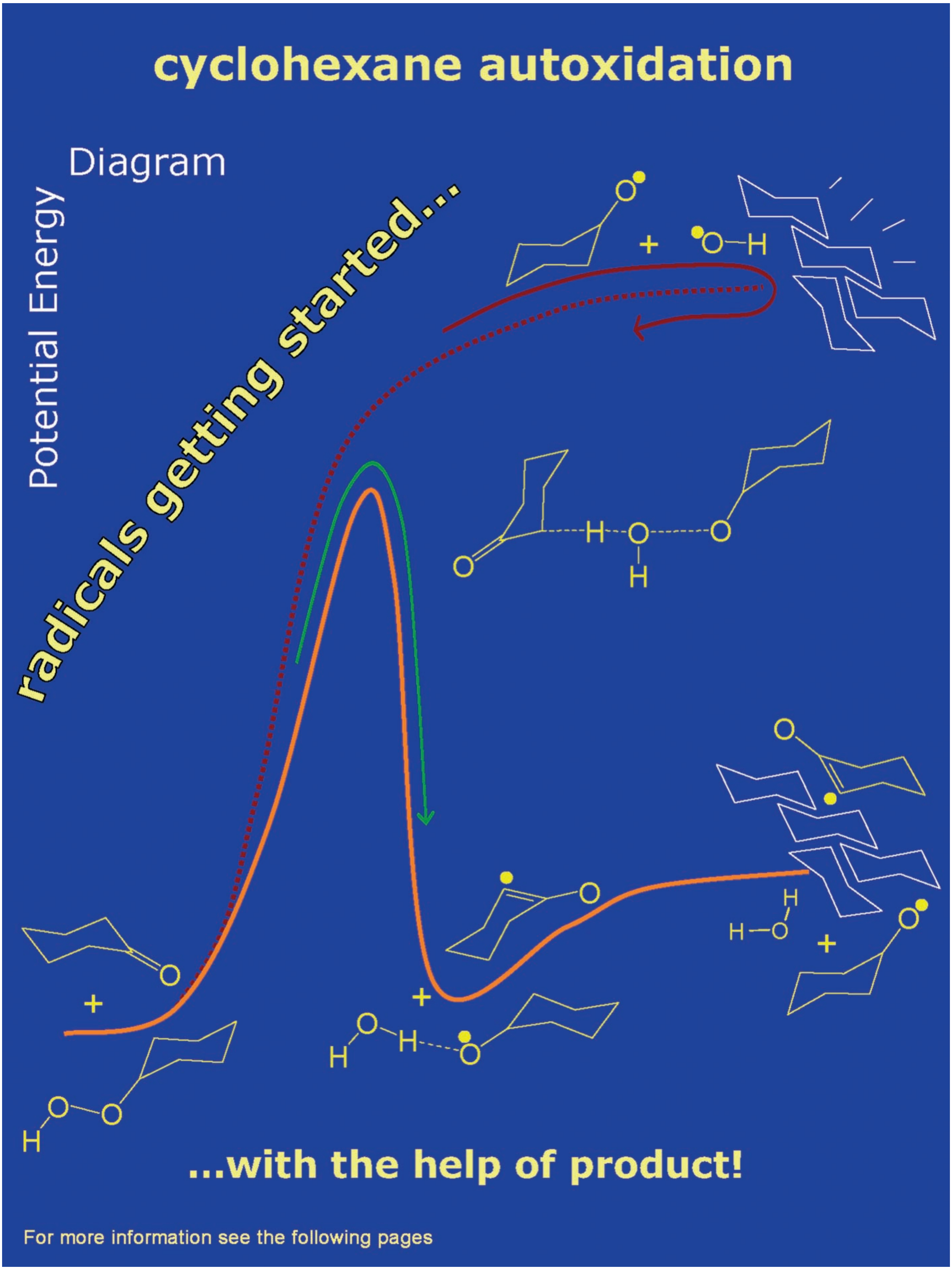
cyclohexane autoxidation
Potential Energy Diagram
radicals getting started...
+
O
H
...with the help of product!
For more information see the following pages

CHEMISTRY
A EUROPEAN JOURNAL

DOI: 10.1002/chem.200600189

To the Core of Autocatalysis in Cyclohexane Autoxidation

Ive Hermans,[a, b] **Pierre A. Jacobs,**[b] **and Jozef Peeters***[a]

Abstract: Despite their industrial importance, the detailed reaction mechanism of autoxidation reactions is still insufficiently known. In this work, complementary experimental and theoretical techniques are employed to address the radical-chain initiation in the autoxidation of cyclohexane with a particular focus on the "lighting-off" of the oxidation by (added) cyclohexanone. We used a newly developed method to quantify the intrinsic rate of chain initiation as well as the rate enhancement by cyclohexanone and several other (oxygenated) molecules. On the basis of first principles, the hitherto assumed perhemiketale mechanism was found to be many orders of magnitude too slow to account for the observed initiation enhancement by the ketone. Instead, it is shown that the pronounced chain-initiation enhancement by the ketone is attributable to a newly proposed concerted reaction between cyclohexyl hydroperoxide and cyclohexanone, in which the $^{\bullet}OH$ radical breaking away from the hydroperoxide abstracts an αH atom from the ketone, thereby energetically assisting in the cleavage of the RO–OH bond. This reaction is highly efficient in generating radicals as it quasi-excludes geminate in-cage recombination. As a result, the ketone oxidation product at a level of 1 mol% increases the initiation rate by one order of magnitude, and so acts as a highly efficient "autocatalyst" in autoxidation reactions. An analogous reaction with cyclohexanol, although estimated to be even faster, has only a marginal effect on the overall kinetics, owing to the fast subsequent formation of $HO_2^{\bullet}$ radicals that very rapidly terminate with other $ROO^{\bullet}$ radicals. Finally, solid evidence is presented that, also in absence of oxygenates, ROOH initiation is actually a bimolecular reaction, involving concerted H abstraction from the alkane substrate by the nascent $^{\bullet}OH$.

Keywords: autoxidation • initiation • kinetics • radicals • thermal rate theory

Introduction

The liquid-phase autoxidation of hydrocarbons, such as cyclohexane, *p*-xylene and cumene, is an important process in the petrochemical value chain.[1–4] The industrial oxidation of cyclohexane, with a capacity of 6×10^6 tons per year, yields cyclohexanone and cyclohexanol, the feedstock chemicals for nylon. The oxidation of *p*-xylene yields terephthalic acid (capacity of 30×10^6 tons per year), a building block for poly(ethylene terephthalate). Likewise, cumene hydroperoxide (capacity 5×10^6 tons per year), derived from the oxidation of cumene, serves as feedstock for both phenol and acetone. Other industrially important autoxidation processes are, for example, the conversion of ethylbenzene to ethylbenzene hydroperoxide (capacity 5×10^6 tons per year), and the oxidation of isobutene to *tert*-butylhydroperoxide (capacity 4×10^6 tons per year). A serious drawback of autoxidation chemistry is the free-radical mechanism, often limiting the product yield because the oxygenated products are oxidised faster than the alkane substrate. For example, the autoxidation of cyclohexane (CyH) is limited to 5% conversion with cyclohexyl hydroperoxide (CyOOH), cyclohexanone (Q=O, Q represents the 1,1-cyclohexylene biradical) and cyclohexanol (CyOH) still constituting the majority of the products.[1–7] At higher conversions, significant amounts of ring-opened byproducts, such as 6-hydroxyhexanoic acid and adipic acid, appear. Although it would be of interest to synthesise adipic acid directly from cyclohexane, carboxylic acids tend to decarboxylate under autoxidation conditions.

---

[a] Dr. I. Hermans, Prof. Dr. J. Peeters
Division of Quantum Chemistry and Physical Chemistry
Department of Chemistry, K.U.Leuven
Celestijnenlaan 200F, 3001 Heverlee (Belgium)
Fax: (+32) 16-327-992
E-mail: jozef.peeters@chem.kuleuven.be

[b] Dr. I. Hermans, Prof. Dr. P. A. Jacobs
Centre for Surface Chemistry and Catalysis
Department of Microbial and Molecular Systems, K.U.Leuven
Kasteelpark Arenberg 23, 3001 Heverlee (Belgium)

Supporting information for this article is available on the WWW under http://www.chemeurj.org/ or from the author.

This results in the appearance of a whole range of C_1–C_5 (di)acids and CO_x, significantly decreasing the selectivity.

The same radical autoxidation chemistry is also known to occur with fats/oils, causing food deterioration. For this reason, antioxidants, such as substituted phenols, are added to (poly)unsaturated fats to prevent their oxidation in air.[8,9] Clearly, a detailed understanding of the autoxidation mechanism would not only be beneficial for industrial process optimisation, or the design of catalysts, but it could also be helpful in preventing harmful radical-chain reactions from starting.

The present contribution focuses on the autoxidation of cyclohexane, a model substrate for other hydrocarbons and a major challenge in its own right.[6] In the autoxidation of CyH, the homolytic dissociation of CyOOH into CyO$^•$ and $^•$OH radicals [Eq. (1)] is considered to be the major chain-initiation reaction, while the mutual reaction of two peroxyl radicals [Eq. (2)] constitutes the chain-termination step.[1–7]

$$\mathrm{CyOOH} \rightarrow \mathrm{CyO}^{\cdot} + {}^{\cdot}\mathrm{OH} \tag{1}$$

$$\mathrm{CyOO}^{\cdot} + \mathrm{CyOO}^{\cdot} \rightarrow \mathrm{CyOH} + \mathrm{Q{=}O} + \mathrm{O_2} \tag{2}$$

CyOOH is produced by fast propagation [Eqs. (3) and (4)]. At a sufficient O_2 pressure, the diffusion-controlled reaction [Eq. (4)] occurs so fast that the reaction given in Equation (3) becomes rate-determining in the overall chain-propagation sequence.[1–7]

$$\mathrm{CyOO}^{\cdot} + \mathrm{CyH} \rightarrow \mathrm{CyOOH} + \mathrm{Cy}^{\cdot} \tag{3}$$

$$\mathrm{Cy}^{\cdot} + \mathrm{O_2} \rightarrow \mathrm{CyOO}^{\cdot} \tag{4}$$

CyOOH can initiate new radical chains, thus causing a steady increase in the oxidation rate. Until recently, the literature failed to explain how the radical-chain reactions are able to produce the major products cyclohexanol and cyclohexanone. It was assumed that the chain termination [Eq. (2)] was the exclusive source of ketone, while additional alcohol could originate by H abstraction from CyH by cyclohexoxy radicals (CyO$^•$) formed in the initiation [Eq. (1)]. However, given the long radical chain length of ≈10–100,[2] it is clear that initiation and termination can indeed account for a minor fraction of the products. This is not compatible with the experimental product distribution: for example, the CyOOH/CyOH/Q=O molar ratio equals 35/35/30 at 4% CyH conversion and 145 °C. Therefore, the bulk of the products should be formed in much faster propagation reactions.

In recent studies of the autoxidation of cyclohexane,[10,11] we identified CyOOH as the key primary product, from which Q=O and CyOH originate by fast subsequent propagation reactions. Indeed, CyOH and Q=O were manifestly shown to be secondary products. We demonstrated, both by state-of-the-art theoretical methodologies[10] and experiments,[11] that cyclohexyl peroxylradicals (CyOO$^•$) not only abstract hydrogen atoms from the substrate molecule (CyH, Scheme 1a), but also, and much more rapidly, the weakly bound αH atom of CyOOH (Scheme 1b). The ratio of the

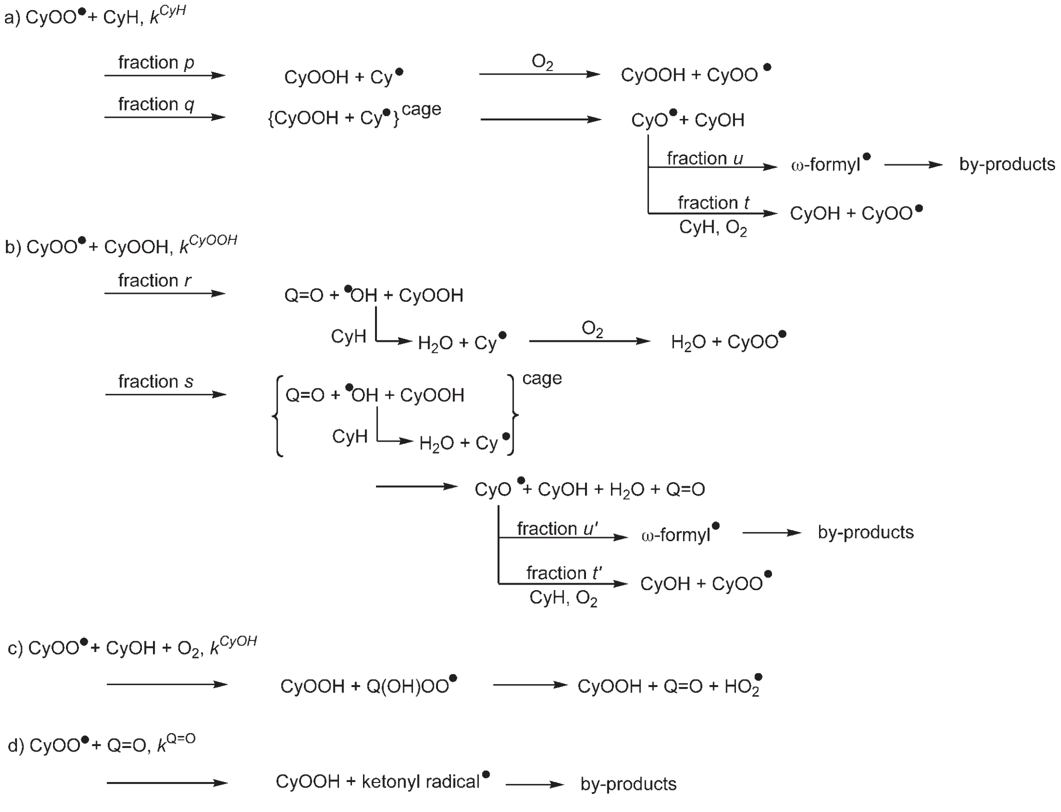

Scheme 1. a)–d) Propagation reactions in the autoxidation of cyclohexane.

propagation rate constants k^{CyOOH}/k^{CyH} was determined to be as high as 55. As is well-established, α-hydroperoxyalkyl radicals, formed here by αH abstraction from CyOOH, are unstable[12] and spontaneously dissociate into ˙OH and Q=O [Eq. (5)] in the absence of any energy barrier.

$$\mathrm{CyOOH + CyOO^{\cdot} \rightarrow Q{=}O + {}^{\cdot}OH + CyOOH} \qquad (5)$$

A subsequent Franck–Rabinowich cage reaction of the products of the CyOOH αH-abstraction was identified as the major source of alcohol CyOH and CyO˙ radicals [Eqs. (6) and (7)] (fraction *s* in Scheme 1b).[10,11]

$$\begin{aligned}&\mathrm{\{Q{=}O{+}{}^{\cdot}OH + CyOOH + CyH\}^{cage} \rightarrow}\\&\qquad\mathrm{\{Q{=}O + H_2O + CyOOH + Cy^{\cdot}\}^{cage}}\end{aligned} \qquad (6)$$

$$\begin{aligned}&\mathrm{\{Q{=}O{+}H_2O + CyOOH + Cy^{\cdot}\}^{cage} \rightarrow}\\&\qquad\mathrm{\{Q{=}O + H_2O + CyO^{\cdot} + CyOH\}^{cage}}\end{aligned} \qquad (7)$$

The competing out-of-cage-diffusion [Eq. (8)] was shown to contribute only 30 % to the CyOOH-propagation flux (fraction *r* in Scheme 1). The high CyOH-formation efficiency of this cage reaction is caused by a nano-sized hotspot,[10] generated by the large amount of released heat (≈60 $\mathrm{kcal\,mol^{-1}}$) of 1) αH abstraction from CyOOH (Scheme 1b),[12] and 2) the subsequent H abstraction from CyH by ˙OH [Eq. (6)].

$$\begin{aligned}&\mathrm{\{Q{=}O{+}H_2O + CyOOH + Cy^{\cdot}\}^{cage} \rightarrow}\\&\qquad\mathrm{Q{=}O + H_2O + CyOOH + Cy^{\cdot}}\end{aligned} \qquad (8)$$

Because 35 % of the CyO˙ coproduct radicals undergo ring-opening by β-C–C cleavage (fraction *u'* in Scheme 1), the cage reaction also accounts for the majority of the (acid) byproducts.[11] An analogous cage reaction can occur after primary H abstraction from CyH (fraction *q* in Scheme 1a). As this cage reaction is not activated, its efficiency is much smaller, so that it contributes only 5 % to the CyH-propagation flux. Nevertheless, this minor reaction channel explains the previously observed direct formation of some CyOH from CyH,[5] which was hitherto not understood. Although the αH abstraction from CyOH by CyOO˙ was found to be somewhat slower than reaction shown in Equation (5), it is still important ($k^{CyOH}/k^{CyH} \approx 10$, Scheme 1). The resulting α-hydroxyalkylperoxyl radical (Q(OH)OO˙) was shown to rapidly equilibrate into Q=O and $\mathrm{HO_2^{\cdot}}$. Because the equilibrium is strongly shifted towards the products, it constitutes another, although minor, ketone source.[13] Q=O is even less reactive than CyOH towards CyOO˙ ($k^{Q=O}/k^{CyH} \approx 5$). Therefore, Q=O can only account for a minor fraction of the byproducts,[11] in contrast to previously published ideas.[1–4]

This contribution focuses on the mechanisms of radical-chain initiation in the autoxidation of cyclohexane. In the literature, it has been recognized that "ketones light-off the reaction"[14] and somehow contribute to its autocatalytic nature. This major issue in alkane autoxidation—which has remained rather enigmatic thus far—is the principal subject of the present work, which aims to unravel the detailed mechanisms of radical-chain initiation by combining complementary experimental and theoretical methods.

Experimental Section

The autoxidation of cyclohexane (50 mL, HPLC-grade) was studied experimentally in a stirred (500 rpm) stainless steel high-pressure Parr reactor (100 mL) at an initial room-temperature pressure of 2.76 MPa of pure oxygen. Prior to each experiment, the reactor wall was passivated by means of a saturated sodium pyrophosphate (p.a.) solution.[15] Acetone (p.a.) was added to the reaction mixture to dissolve all products. The reaction products were quantified by GC-FID, after the addition of an external standard (1-heptanol, 99.9 %) and the silylating agent *N*-methyl-*N*-(trimethylsilyl)-trifluoroacetamide (MSTFA); the injection temperature was set to 150 °C. Peak areas were corrected for sensitivity differences by calibration.

Computational methods: Quantum-chemical calculations to construct potential energy surfaces (PES), were carried out with the GAUSSIAN 03 program.[16] At the DFT level, we used the Becke three-parameter hybrid exchange functional, combined with the Lee–Yang–Parr nonlocal correlation functional B3LYP-DFT.[17] High-level, single-point G2M calculations[18] were performed on the B3LYP-DFT geometries to improve the relative energies. Thermal rate constants were calculated with multiconformer transition state theory (MC-TST),[19–21] or its variational counterpart,[20] incorporating tunnelling corrections adopting the asymmetric Eckart potential approach,[22] and describing partition functions of one- and two-dimensional hindered internal rotation modes by appropriate approximations.[23]

Results and Discussion

Autocatalysis caught in the act: Figure 1 depicts the product concentrations as a function of time for cyclohexane autoxidation at 145 °C.

Based on the recently derived mechanism (Scheme 1),[10,11] the rate of CyH oxidation, or of formation of oxygenated products, P, for conversions ≤3 %, can be calculated with Equation (9).

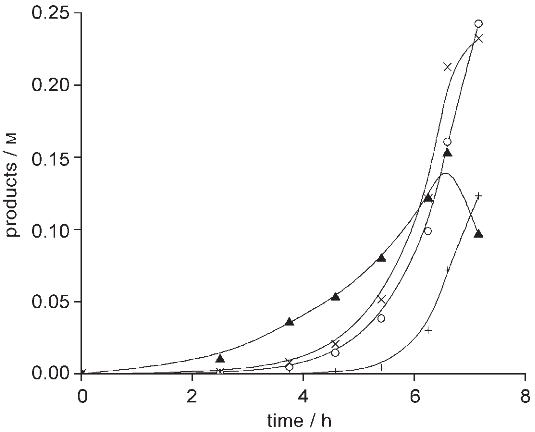

Figure 1. Concentrations as function of time of the oxidation products CyOOH (▲), CyOH (×), Q=O (○) and ring-opened byproducts (+) during CyH autoxidation at 145 °C.

$$\frac{\mathrm{d}\sum[\mathrm{P}]}{\mathrm{d}t} = [\mathrm{CyOO}^{\bullet}]\{(1+qt)k^{\mathrm{CyH}}[\mathrm{CyH}] + (1+st')k^{\mathrm{CyOOH}}[\mathrm{CyOOH}]\} \tag{9}$$

The values of the coefficients $(1+qt)$ and $(1+st')$ and the ratio $k^{\mathrm{CyOOH}}/k^{\mathrm{CyH}}$ at 145 °C, derived from experimental data[10] are equal to 1.03, 1.36 and 55, respectively. With the radical quasi-steady-state expression [Eq. (10)],[24] Equation (9) rearranges into Equation (11), in which k_{init} represents the apparent (pseudo-)first-order rate constant for CyOOH dissociation.

$$[\mathrm{CyOO}^{\bullet}]^{\mathrm{QSS}} = \sqrt{\frac{k_{\mathrm{init}}[\mathrm{CyOOH}]}{k_{\mathrm{term}}}} \tag{10}$$

$$k^{\mathrm{CyH}}\sqrt{\frac{k_{\mathrm{init}}}{k_{\mathrm{term}}}} = \frac{1}{\sqrt{[\mathrm{CyOOH}]}}\,\frac{\mathrm{d}\sum[\mathrm{P}]/\mathrm{d}t}{1.03[\mathrm{CyH}]+73.5[\mathrm{CyOOH}]} \tag{11}$$

The rate coefficient k^{CyH} at 145 °C was taken to be equal to $7.8\,\mathrm{M}^{-1}\mathrm{s}^{-1}$, that is, equal to the average of the literature value ($11.4\,\mathrm{M}^{-1}\mathrm{s}^{-1}$)[3] and our theoretical prediction ($4.3\,\mathrm{M}^{-1}\mathrm{s}^{-1}$);[10] its precise value is of little importance for what follows. In Figure 2a, the $k_{\mathrm{init}}/k_{\mathrm{term}}$ ratio obtained from Equation (11) is plotted against Σ[P] for the 145 °C CyH autoxidation. It is striking that the $k_{\mathrm{init}}/k_{\mathrm{term}}$ increases by an order of magnitude as the reaction progresses and products gradually build up, indicating that one of the oxygenated products strongly enhances the initiation. The shape of the curve points to the secondary nature of this product, namely, Q=O or CyOH. To identify the product causing autocatalysis, 1 mol % of cyclohexanone or cyclohexanol was initially added to the CyH autoxidation at 145 °C. Whereas alcohol addition had only a marginal effect (Figure 3a), cyclohexanone (Figure 3b) was indeed found to light-off the reaction, and to increase the $k_{\mathrm{init}}/k_{\mathrm{term}}$ ratio by more than a factor of ten compared to the initial value (Figure 2b).

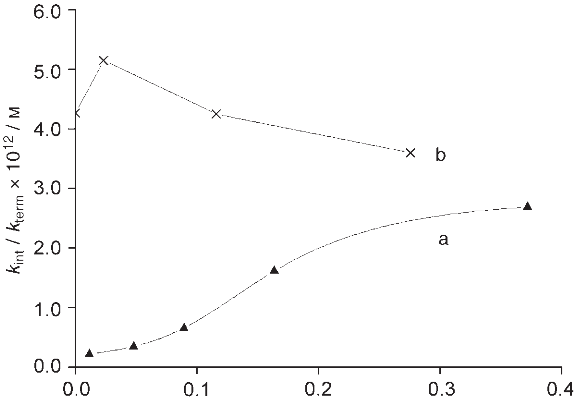

Figure 2. Plot of $k_{\mathrm{init}}/k_{\mathrm{term}}$ against the sum of oxygenated products, Σ[P], a) during CyH autoxidation at 145 °C, and b) when initially 1 mol % ketone was added.

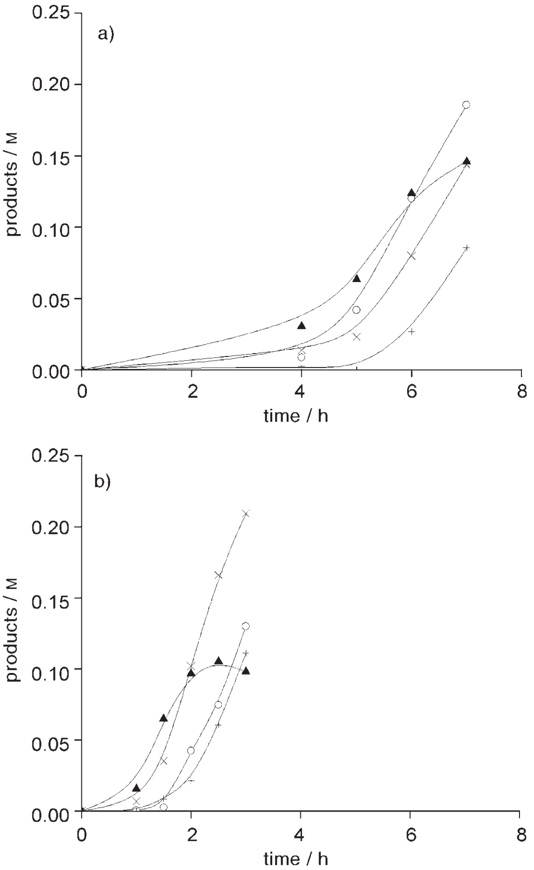

Figure 3. Concentrations of the CyH autoxidation products as a function of time at 145 °C after initial addition of 1 mol % CyOH (a) or Q=O (b); CyOOH (▲), CyOH (×), Q=O (○) and ring-opened byproducts (+).

However, at higher conversions (>2 %), the enhancement of the initiation in the autoxidation appears to be counteracted by another phenomenon because $k_{\mathrm{init}}/k_{\mathrm{term}}$ is found to approach an asymptotic value of $\approx 3\times10^{-12}\,\mathrm{M}$ (Figure 2). This levelling-off is most probably caused by $\mathrm{HO_2}^{\bullet}$ radicals formed in the CyOH co-oxidation (Scheme 1c). Indeed, the termination rate constant for $\mathrm{HO_2}^{\bullet}+\mathrm{CyOO}^{\bullet}$ ($\approx 2.0\times10^{9}\,\mathrm{M}^{-1}\mathrm{s}^{-1}$),[25] is several orders of magnitude larger than the mutual $\mathrm{CyOO}^{\bullet}$ termination rate constant ($k_{\mathrm{term}}=4.2\times10^{6}\,\mathrm{M}^{-1}\mathrm{s}^{-1}$).[3] Note that the higher ketone production in the presence of 1 mol % initial CyOH (Figure 3a), as compared to the case with pure CyH (Figure 1), is readily rationalised by the fast co-oxidation of CyOH to Q=O (Scheme 1c). The lower *net* production of ketone and the higher yield of byproducts when 1 mol % Q=O is added (Figure 3b) is attributed to the co-oxidation of the initial ketone (Scheme 1d), whereas the lower CyOOH yield must be ascribed to an increase of the $k^{\mathrm{CyOOH}}/k^{\mathrm{CyH}}$ ratio as a result of Q=O addition.

Quantification of the initiation enhancement: To decouple the initiation enhancement—most likely by cyclohexanone—and the enhanced termination by $\mathrm{HO_2}^{\bullet}$ radicals from

CyOH co-oxidation, we developed a procedure to exclusively quantify the enhanced initiation. At very low conversions, namely $\Delta[CyH]/[CyH] < 0.2\,\%$, for which [CyOOH] and [CyOH] are both below 0.1 mol%, $HO_2^{\bullet}$ formation by CyOH co-oxidation (Scheme 1c), and CyOOH removal (Scheme 1b) can be neglected. The CyOOH formation rate can thus be expressed, within ±10%, by Equation (12) in which p represents the CyOOH yield of the primary propagation step (Scheme 1a; $p = 0.95$ at 145 °C).[10]

$$\frac{d[CyOOH]}{dt} \approx p\,k^{CyH}\,[CyOO^{\cdot}]\,[CyH] \tag{12}$$

In Equation (12), the time-dependent $CyOO^{\bullet}$ concentration can be substituted by its quasi-steady-state expression, [Eq. (10)],[24] resulting in the differential Equation (13), which upon integration yields Equation (14)

$$d[CyOOH]/dt = p\,k^{CyH}\,(k_{init}/k_{term})^{0.5}\,[CyH]\,[CyOOH] \tag{13}$$

$$[CyOOH](t) - [CyOOH]^0 = \left(\frac{C}{2}\right)^2 t^2 + C\sqrt{[CyOOH]^0}\,t \tag{14}$$

In Equation (14), $C = p\,k^{CyH}[CyH]\,(k_{init}/k_{term})^{0.5}$ and $[CyOOH]^0$ is the initial concentration at $t = 0$; Equation (14) is only valid when $[CyOOH]^0$ is sufficient to establish the $CyOO^{\bullet}$ quasi-steady state[24] according to Equation (10) from the very beginning ($t = 0$) of the autoxidation.

On the other hand, the O_2 consumption rate at very low conversions can be written as Equation (15), in which n_{O_2} is the total number of moles of oxygen in the reactor and V_{liq} is the liquid volume (in which the reaction occurs).[26]

$$-\frac{1}{V_{liq}}\frac{dn_{O_2}}{dt} \approx k^{CyH}\,[CyOO^{\cdot}]\,[CyH] \tag{15}$$

Thus, the oxygen consumption and the CyOOH production follow an identical time dependence [Eq. (16)].

$$\frac{n_{O_2}{}^0}{V_{liq}} - \frac{n_{O_2}(t)}{V_{liq}} = \frac{1}{p}\left(\frac{C}{2}\right)^2 t^2 + \frac{1}{p}\,C\,\sqrt{[CyOOH]^0}\,t \tag{16}$$

Fitting of the initial oxygen consumption at a conversion below 0.2% to a quadratic equation in t, allows the evaluation of parameter C. With $k^{CyH} = 9.5\times10^9\,\text{M}^{-1}\text{s}^{-1}\exp(-17.3\,\text{kcal mol}^{-1}/RT)$,[3,10] the k_{init}/k_{term} can be derived. This was carried out with cyclohexane that initially contained 0.46 mM CyOOH to assure the quasi-steady state[24] from the very beginning of the O_2 consumption. This CyOOH solution was prepared by the dilution of a CyH autoxidation mixture of low conversion (<0.5%) in which CyOOH is by far the predominant product (see Figure 1). The k_{init}/k_{term} ratios found for various initially added cyclohexanone concentrations are displayed in Figure 4, showing that k_{init} is actually made up of a sum, $k_{diss} + k_{enh}^{Q=O}[Q{=}O]$, with k_{diss} the intrinsic dissociation rate constant of CyOOH [Eq. (1)], and $k_{enh}^{Q=O}$ the bimolecular rate constant for a cyclohexanone-enhanced CyOOH dissociation process. The k_{init}/k_{term} ratios are in rather good agreement with those determined from Equation (11) (Figure 2). For $k_{term} = 4.2\times10^6\,\text{M}^{-1}\text{s}^{-1}$,[3] a value of $k_{diss} = 1.8\times10^{-6}\,\text{s}^{-1}$ is found from the intercept and $k_{enh}^{Q=O} = 1.9\times10^{-4}\,\text{M}^{-1}\text{s}^{-1}$ from the slope of the straight line in Figure 4. The ratio $\{k_{enh}^{Q=O}x[Q{=}O]\}/k_{diss}\}$ at 145 °C is $1.0\times10^2\,\text{M}^{-1}\times[Q{=}O]$, revealing that the cyclohexanone-enhanced initiation already rivals the "pure" initiation when $[Q{=}O] \geq 10$ mM. This value is reached in a normal autoxidation at CyH conversions as low as 1%.

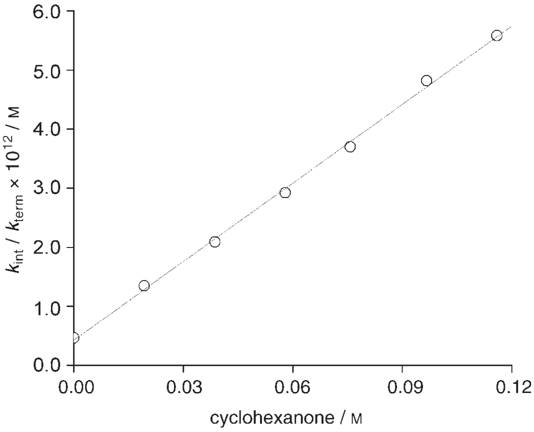

Figure 4. Change of the k_{init}/k_{term} ratio against initially added cyclohexanone at 145 °C.

This method was also used to determine the initiation enhancement by several other (oxygenated) molecules (Table 1). Apparently, not only cyclohexanone but also other oxygenated compounds significantly enhance the initiation rate. Therefore, the accuracy of the data for k_{enh} and k_{diss} reported above might be questioned because, in this first approximation [Eq. (16)], the possibility of initiation enhancement by CyOOH itself was not considered. Moreover, the O_2 consumption in the fast CyOOH propagation (Scheme 1b) was neglected, which will affect dn_{O_2}/dt the most at larger t, at which CyOOH consumption can no longer be neglected. Therefore, in a second approximation, we measured $k_{enh}^{Q=O}$, k_{enh}^{CyOOH} as well as k_{diss}, taking into account the oxygen consumption in the CyOOH propagation. To do this, the change in time of the CyOOH concentration is derived from the dn_{O_2}/dt data,[26] by means of the integrated form of Equation (17).[27]

Table 1. Rate constants, k_{enh}^{X} for the enhancement of the dissociation of CyOOH by several oxygenated compounds, X, measured at 145 °C.

Compound	$k_{enh}^{X}\times10^{-5}$ [$\text{M}^{-1}\text{s}^{-1}$]	Compound	$k_{enh}^{X}\times10^{-5}$ [$\text{M}^{-1}\text{s}^{-1}$]
cyclohexanone	19.0	cyclopentanone	7.8
caprolactone	3.1	ethylene carbonate	2.2
1-methylcyclohexanol	1.0	benzoic acid	3.7
butyric acid	38.0		

$$\frac{d[\mathrm{CyOOH}]}{dt} = -p\left\{1 - \frac{(p+s)k^{\mathrm{CyOOH}}\,[\mathrm{CyOOH}](t)}{p\,k^{\mathrm{CyH}}\,[\mathrm{CyH}]}\right\}\frac{1}{V_{\mathrm{liq}}}\frac{dn_{\mathrm{O_2}}}{dt} \tag{17}$$

An initial estimation for [CyOOH](t) is given by Equation (18):

$$[\mathrm{CyOOH}]^0 + \frac{p}{V_{\mathrm{liq}}}\{n_{\mathrm{O_2}}{}^0 - n_{\mathrm{O_2}}{}^0(t)\} \tag{18}$$

Based on our reaction mechanism, the CyOOH concentration change is described by Equation (19),[28] taking into account the possible enhancement of the initiation by both CyOOH and Q=O.

$$\sqrt{[\mathrm{CyOOH}]} + \sqrt{[\mathrm{CyOOH}] + \frac{k_{\mathrm{init}}}{k_{\mathrm{enh}}^{\mathrm{CyOOH}}}} = \left\{\sqrt{[\mathrm{CyOOH}]} + \sqrt{[\mathrm{CyOOH}]^0 + \frac{k_{\mathrm{init}}}{k_{\mathrm{enh}}^{\mathrm{CyOOH}}}}\right\}\exp\left(k^{\mathrm{CyH}}\,[\mathrm{CyH}]\sqrt{\left(\frac{k_{\mathrm{enh}}^{\mathrm{CyOOH}}}{k_{\mathrm{term}}}\right)}\,\frac{t}{2}\right)$$
$$\text{with } k_{\mathrm{init}} = k_{\mathrm{diss}} + k_{\mathrm{enh}}^{\mathrm{Q=O}}\,[\mathrm{Q{=}O}] \tag{19}$$

The CyOOH profiles obtained this way [Eq. (19)] are plotted in Figure 5, together with the experimental CyOOH data, derived from the O_2 consumption [Eq. (17)]. The sum of squares of the differences between the experimental data and the theoretical prediction was minimized by combining the data of two independent experiments (Figure 5).

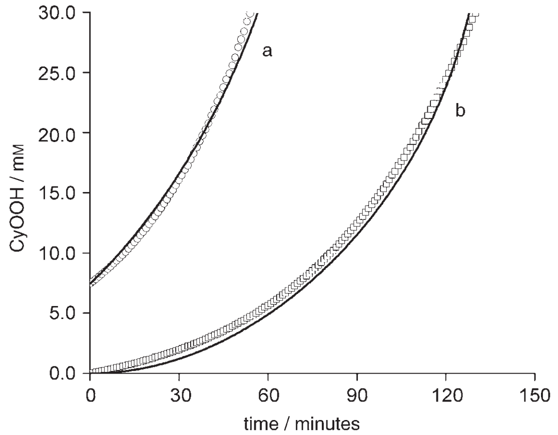

Figure 5. Comparison of the experimental (open symbols) and theoretical (solid lines) [CyOOH](t) profiles at 145 °C for two initial conditions. a) $[\mathrm{CyOOH}]^0 = 0.08$ mol %, [Q=O] = 0.04 mol %. b) $[\mathrm{CyOOH}]^0$ and [Q=O] < 0.01 mol %.

This rigorous evaluation reveals that CyOOH does not significantly enhance its own homolytic dissociation ($k_{\mathrm{enh}}^{\mathrm{CyOOH}} = 6.0\times10^{-6}\,\mathrm{M^{-1}s^{-1}}$). Nevertheless, the values $k_{\mathrm{enh}}^{\mathrm{Q=O}} = 1.0\times10^{-4}\,\mathrm{M^{-1}s^{-1}}$ and $k_{\mathrm{diss}} = 1.0\times10^{-6}\,\mathrm{s^{-1}}$, derived according to the second approximation, are each ≈40 % smaller than the first-approximation estimates of $1.9\times10^{-4}\,\mathrm{M^{-1}s^{-1}}$ and $1.8\times10^{-6}\,\mathrm{s^{-1}}$, respectively. Indeed, it is expected that the first approximation overestimates both the intrinsic dissociation rate and the Q=O contribution as the neglected CyOOH propagation will increase the curvature of the $n_{\mathrm{O_2}}(t)$ profile. It follows that the k_{enh} data (Table 1), although slightly overestimated, still represent fair first approximations. In any case, the relative values should be reliable.

It is interesting to note that, although the experimentally determined "intrinsic" CyOOH dissociation rate constant ($k_{\mathrm{diss}} = 1.0\times10^{-6}\,\mathrm{s^{-1}}$) is one order of magnitude smaller than the reported CyOOH initiation rate in CyH ($\approx 2.2\times10^{-5}\,\mathrm{s^{-1}}$), it approaches the value for *tert*-butylhydroperoxide initiation in *n*-octane ($5.1\times10^{-6}\,\mathrm{s^{-1}}$).[3] Clearly, the "homolytic dissociation" rates measured under autoxidation conditions, even though "extrapolated to infinite dilution", contain contributions of enhanced initiation by numerous oxygenated compounds, particularly ketones. Such ketones are readily generated from secondary hydroperoxides, such as CyOOH, by fast αH abstraction, even if only added in a few percent (cf. $k^{\mathrm{CyOOH}}/k^{\mathrm{CyH}} \approx 55$). However, in the case of *tert*-butylhydroperoxide (in *n*-octane), there is no αH atom left, so that ketones will appear more slowly via oxidation of the *n*-octane solvent. Therefore, a more accurate measurement of the intrinsic dissociation rate constant is expected in the latter case.

True catalysis against chemical reaction: Recently, we proposed[29] novel initiation catalysts, X, such as perfluorodecaline, which are able to form hydrogen bonds with the $^{\bullet}$OH that is breaking away from CyO–OH [Reaction (20)]:

$$\mathrm{CyOOH} + \mathrm{X} \rightarrow \mathrm{CyO}^{\bullet} + \mathrm{X}\cdots\mathrm{HO}^{\bullet} \rightarrow \mathrm{CyO}^{\bullet} + \mathrm{X} + \mathrm{HO}^{\bullet} \tag{20}$$

This stabilization substantially decreases the rate-determining initiation barrier. The hydrogen-bonded complex, X···HO$^{\bullet}$, rapidly decomposes to yield X and HO$^{\bullet}$. Given the computed hydrogen-bond strengths between HO$^{\bullet}$ and several oxygenated compounds (see Table 2), the same catalytic mechanism should, in principle, be possible with, for example, ketones, alcohols and other oxygenated compounds.

To examine the feasibility of such a dissociation of CyOOH assisted by hydrogen bonding to Q=O, we estimated the thermal rate constant for this process on the basis of variational TST theory.[30] The upper-limit value ($1.8\times10^{-5}\,\mathrm{M^{-1}s^{-1}}$) turns out to be an order of magnitude too small, making this mechanism unlikely. Moreover, such a mechanism does not explain why caprolactone, among others, is much less efficient than cyclohexanone, despite its stronger hydrogen bond with $^{\bullet}$OH. However, the predicted rate constant for hydrogen-bond-assisted initiation ($1.8\times10^{-5}\,\mathrm{M^{-1}s^{-1}}$) is consistent with the experimental $k_{\mathrm{enh}}^{\mathrm{X}}$ of, for example, 1-methylcyclohexanol ($1.0\times10^{-5}\,\mathrm{M^{-1}s^{-1}}$) and benzoic acid ($3.7\times10^{-5}\,\mathrm{M^{-1}s^{-1}}$).

In the literature, the remarkable autocatalytic effect of cyclohexanone was hitherto attributed to the formation of a

Table 2. Hydrogen-bond strengths [zero-point energy-corrected, in kcal mol^{-1}] between HO$^•$ and several oxygenated compounds, calculated at the B3LYP-DFT[17] and G2M[18] level.

Compound	B3LYP/6-311++G(d,p)	G2M[a]
formaldehyde	3.4	3.6
acetaldehyde	4.25	4.6
acetone	4.95	5.2
cyclopentanone	5.2	–
cyclohexanone	5.5	–
3-pentanone	5.0	–
methanol	5.4	4.75
isopropylalcohol	5.4	5.3
tert-butanol	5.5	–
cyclohexanol	5.5	–
ethylene carbonate	4.6	–
caprolactone	6.1	–
ethyl hydroperoxide	4.1	4.7

[a] G2M refers to E[CCSD(T)/6-311+G(d,p)//B3LYP/6-311++G(d,p)]+{E[MP2/6-311++G(3df,3pd)//B3LYP/6-311++G(d,p)]−E[MP2/6-311+G(d,p)//B3LYP/6-311++G(d,p)]}+ZPE[B3LYP/6-311++G(d,p)].

perhemiketale structure out of CyOOH and Q=O (Scheme 2).[1–3] Such a perhemiketale would undergo O−O cleavage more easily than CyOOH, and thus enhance the initiation rate. However, such a bimolecular reaction between closed-shell molecules, proceeding through a rigid transition state, is expected to be very slow in the nonpolar solvent CyH. The B3LYP-DFT/6-311++G(d,p) barrier was found to be more than 30 kcal mol^{-1} for $(CH_3)_2C{=}O + CH_3OOH$, while the TST frequency-factor was estimated to be as low as $2\times10^{6}\,\text{M}^{-1}\text{s}^{-1}$, resulting in a rate constant at 145 °C of, at most, $10^{-9}\,\text{M}^{-1}\text{s}^{-1}$, which is five orders of magnitude too low compared to the experimental value of $1.0\times10^{-4}\,\text{M}^{-1}\text{s}^{-1}$ given above.

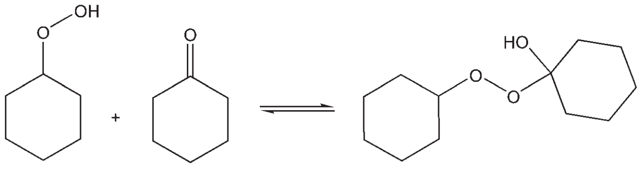

Scheme 2.

Moreover, such perhemiketale formation is excluded for molecules such as ethylene carbonate ($\Delta_rH = +13.0$ kcal mol^{-1}), caprolactone ($\Delta_rH = +6.6$ kcal mol^{-1}) or butyric acid ($\Delta_rH = 6.3$ kcal mol^{-1}), some of which enhance the initiation rate even more than Q=O (Table 1). Therefore, we have to conclude that the perhemiketale hypothesis is unable to explain the experimental observations.

Initiation enhanced by concerted hydrogen abstraction

A new autocatalytic mechanism: After exploring several mechanisms involving pre-reaction complexes to explain the experimental $k_{\text{enh}}^{\text{Q=O}}$ data, and rejecting them for being too slow, we finally identified and theoretically characterised a concerted reaction of CyOOH with Q=O that does match the measured rate. In this process, the $^•$OH that breaks away from CyOOH abstracts a weakly bound αH atom from Q=O (BDE only 87 kcal mol^{-1})[31] to form the much more strongly bound H−OH molecule (BDE = 118 kcal mol^{-1}). The released 31 kcal mol^{-1} assists in the further breaking of the O−O hydroperoxide bond (40 kcal mol^{-1}). Indeed, we were able to locate a TS for this reaction that lies only 27.7 kcal mol^{-1} above the reactants (UB3LYP/6-311++G(df,pd)//UB3LYP/6-31G(d,p) level). In this TS, the OOH group of CyOOH is equatorial and an axial αH atom is abstracted from Q=O (Figure 6). The 27.7 kcal mol^{-1} energy barrier is far below the 40 kcal mol^{-1} barrier for the intrinsic CyOOH homolysis [Eq. (1)]; moreover, and equally important, this TS is a very loose structure, entailing a high frequency factor. The O−O bond is already enlarged from 1.46 to 2.04 Å in the TS, indicating that the $^•$OH radical is almost free from the CyO$^•$ moiety. This is also reflected by the high (imaginary) reaction-coordinate frequency of 1377 cm^{-1}, close to that for H abstraction by a free $^•$OH radical.[32]

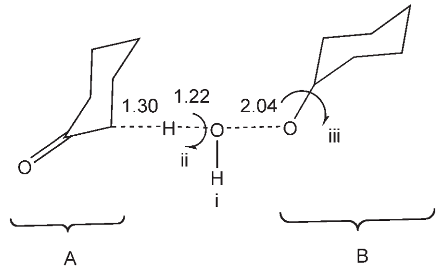

Figure 6. Lowest TS conformer in the hydrogen-abstraction-enhanced initiation of CyOOH by Q=O, optimised at the UB3LYP/6-31G(d,p)-level. Critical coordinates are given in Å. The important internal rotations i, ii and iii are indicated (see text).

The MC-TST rate constant[21] of this reaction can be calculated by Equation (21), in which k_b and h refer to Boltzmann's constant and Planck's constant, respectively; Q_i^{TS} is the partition function of the TS conformer i, lying above the lowest reactant conformer set by the value of E_i^0; Q_j^{CyOOH} is the partition function of CyOOH conformer j, lying above the lowest reactant conformer by an energy of ε_j.

$$k_{\text{enh}}^{\text{Q=O}}(\text{TST}) = \frac{k_b T}{h}\,\frac{\sum_i Q_i^{\text{TS}} \exp(-E_i^0/k_b T)}{\left\{\sum_j Q_j^{\text{CyOOH}} \exp(-\varepsilon_j/k_b T)\right\} Q^{Q=O}} \tag{21}$$

Indeed, a thermal population weighted sum must be taken over all states.[21] Likewise, $Q^{\text{Q=O}}$ is the partition function of Q=O. In this calculation, three internal TS modes, (i, ii and iii in Figure 6), should be treated as quasi-free one-dimensional internal rotations[23] owing to the loose structure of the TS. Internal rotation i is the movement of the H atom of CyOOH around the almost co-linear C-H-O-O axis, with a relative moment of inertia $I_{\mathrm{m,i}}=0.96\,\text{amu}\,\text{Å}^2$. The partition function for this free internal rotation (Q_{fr}) is 7.2, whereas the harmonic oscillator approximation (HOA) for the "vibration" frequency $\nu=189\,\text{cm}^{-1}$[30] gives $Q_{\mathrm{hoa}}=2.1$. Still, the two values could be consistent, provided the H atom can occupy three nearly equivalent equilibrium positions around the O–O axis, which then must be counted as three distinct rotamers in a HOA-MC-TST calculation. Internal rotation ii is the counter-rotation of moieties A and B (Figure 6) around the C-H-O-O axis. The relative moment of inertia for this motion is $I_{\mathrm{m,ii}}\approx 220\,\text{amu}\,\text{Å}^2$, which gives $Q_{\mathrm{fr}}=110$, whereas $Q_{\mathrm{hoa}}=27.3$ for $\nu=10.8\,\text{cm}^{-1}$.[30] Again, these results could still be compatible, as also in this case three equivalent rotational conformers might have to be considered in the HOA. Internal rotation iii is the rotation of moiety B around its O–Cy axis, with counter-rotation of the rest of the TS (Figure 6). Its $I_{\mathrm{m,iii}}$ is estimated to be $\approx 95\,\text{amu}\,\text{Å}^2$, such that $Q_{\mathrm{fr}}=72$, whereas the HOA value $Q_{\mathrm{hoa}}=6.1$ for $\nu=52\,\text{cm}^{-1}$.[30] Thus, Q_{fr} for internal rotation iii remains about four times larger than the harmonic vibration approximation, even accounting for three quasi-equivalent rotamers in the HOA. Thus, the internal partition function of the TS with appropriate treatment of the internal rotors is at least six times that for the crude HOA approximation. For the CyOOH reactant (with OOH equatorial), the partition function was summed over all twelve rotamers, each weighted by their relative-energy function $\exp(-\varepsilon_j/k_{\mathrm{b}}T)$. Accounting for the reaction-path degeneracy of 2 (two equivalent axial αH atoms), and a small-curvature tunnelling correction[22] of 3.0 at 145 °C for an asymmetric-Eckart potential, one obtains a TST frequency factor of $\approx 1.6\times10^{10}\,\text{M}^{-1}\,\text{s}^{-1}$. Given the barrier of $E^{\mathrm{o}}=27.7\,\text{kcal}\,\text{mol}^{-1}$, the TST rate coefficient is finally evaluated to be $k_{\mathrm{enh}}^{\mathrm{Q=O}}(\mathrm{TST})\approx 6.0\times10^{-5}\,\text{M}^{-1}\,\text{s}^{-1}$, which includes minor routes through a TS at 29.6 kcal mol^{-1} in which the equatorial α hydrogens are abstracted from Q=O. This result, derived entirely from first principles, is close to the experimental value of $1.0\times10^{-4}\,\text{M}^{-1}\,\text{s}^{-1}$. It should be noted, however, that the UB3LYP/6-311++G(df,pd)//UB3LYP/6-31G(d,p) method used to evaluate the energy barriers—although agreeing within ±0.2 kcal mol^{-1} with the higher UB3LYP/6-311++G(df,pd) level for smaller analogous reaction systems—might generate errors of 1 kcal mol^{-1}, entailing an error factor of four on the calculated rate coefficient. Interestingly, the energy barrier for the analogous CyOOH+cyclopentanone reaction was found to be 0.6 kcal mol^{-1} higher than for cyclohexanone, such that $k_{\mathrm{enh}}(145\,°\mathrm{C})$ for cyclopentanone is expected to be half as large, in excellent agreement with the experimental data in Table 1.

Thus, we now have solid complementary experimental and theoretical evidence that CyOOH dissociation enhanced by concerted H abstraction from ketones is a predominant, although hitherto overlooked, initiation process in CyH autoxidation.

Reaction dynamics: An important feature of the newly proposed Q=O-assisted initiation is the shape of the PES (Figure 7). In contrast to the classical, unimolecular homolytic dissociation of CyOOH, the potential energy in the hydrogen-abstraction-enhanced initiation decreases sharply once the TS evolves into reaction products. In the TS, the $^{\bullet}$OH originating from CyO–OH already forms a hydrogen bond with the CyO$^{\bullet}$ moiety ($^{\bullet}$OH···O distance = 2.1 Å). Therefore, the TS connects the reactants, CyOOH+Q=O, with the hydrogen-bonded CyO$^{\bullet}$···HOH complex and the $^{\bullet}$Q$_{-\alpha\mathrm{H}}$=O ketonyl radical (i.e., Q=O minus an αH) as primary products, entailing a potential energy drop from 27.7 to 3.4 kcal mol^{-1}, both relative to the reactants. The large energy release of ≈24 kcal mol^{-1} will be imparted to translational separation of the CyO$^{\bullet}$···HOH and ketonyl radical products. This dynamically forced repulsion will reduce the fraction of radicals that can undergo geminate combination in the Franck–Rabinowich solvent cage[33] and instead greatly assist their diffusion out of the cage, allowing them effectively to initiate new radical chains.

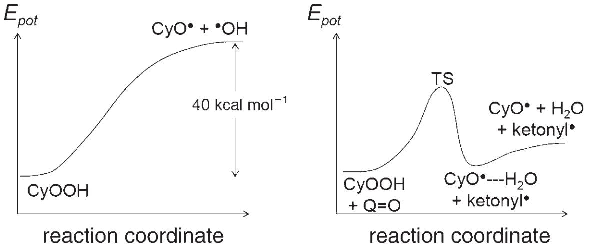

Figure 7. Shape of the PES for the unimolecular homolytic dissociation of CyOOH (left), and the newly proposed Q=O enhanced initiation reaction (right).

Indeed, for the classical initiation mechanism, one needs to consider three elementary reaction steps [Eqs. (22)–(24)].

$$\{\mathrm{CyOOH}\}^{\mathrm{CyH}} \rightarrow \{\mathrm{CyO}^{\bullet} + {}^{\bullet}\mathrm{OH}\}^{\mathrm{CyH}} \tag{22}$$

$$\{\mathrm{CyO}^{\bullet} + {}^{\bullet}\mathrm{OH}\}^{\mathrm{CyH}} \rightarrow \{\mathrm{CyOOH}\}^{\mathrm{CyH}} \tag{23}$$

$$\{\mathrm{CyO}^{\bullet} + {}^{\bullet}\mathrm{OH}\}^{\mathrm{CyH}} \rightarrow \mathrm{CyO}^{\bullet} + {}^{\bullet}\mathrm{OH} \tag{24}$$

The "geminate" in-cage recombination [Eq. (23)] of the nascent radicals, $\{\mathrm{CyO}^{\bullet}+{}^{\bullet}\mathrm{OH}\}^{\mathrm{CyH}}$, should easily outrun their diffusion out of the cage [Eq. (24)], thus seriously reducing the initiation efficiency as compared to the gas phase. In the concerted αH-abstraction-enhanced mechanism, the initiation efficiency is boosted as its dynamics forces the nascent radicals apart. Moreover, the $^{\bullet}$Q$_{-\alpha\mathrm{H}}$=O ketonyl radical is stabilized by vinoxy-type resonance (e.g., O=CH–CH$_2^{\bullet}$⇔$^{\bullet}$O–CH=CH$_2$), which is well-known to reduce radical reactivity; for instance, acetonyl (2-methylvinoxy, $\mathrm{CH_3C(O)CH_2^{\bullet}}$) combines nearly ten times slower with $\mathrm{O_2}$ than the corresponding $\mathrm{CH_3CH_2CH_2^{\bullet}}$ alkyl radical.[34] Last, but not least, the 4.0 Debye large dipole moment of the ketonyl radical (UB3LYP/6-311++G(df,pd)//UB3LYP/6-31G(d,p)-level) will cause extensive solvation by CyH molecules, thus effectively shielding its O=C-CH$^•$ radical centre from the geminate CyO$^•$ radical.

Chain-initiation enhancement by other molecules produced in the autoxidation of CyH: Clearly, other molecules that have (weak) C–H bonds might also similarly enhance chain initiation. Table 3 summarizes the results of B3LYP-DFT calculations on molecules present in the CyH autoxidation mixture.

Table 3. Reaction barriers, zero-point energy-corrected and imaginary reaction coordinate frequencies, ν_{RC}, for the (α)H-abstraction-enhanced initiation of CyOOH by several molecules present in the CyH autoxidation, calculated at the UB3LYP/6-311++G(df,pd)//UB3LYP/6-31G(d,p)-level.

Compound	Barrier [kcal mol^{-1}][a]	ν_{RC} [i×cm^{-1}][a]
Q=O	27.7/29.6	1377/1356
CyOH	24.5/24.2	1018/1037
CyOOH	24.8/25.3	966/967
CyH	28.8/28.1	1168/1181

[a] Axial H atom/equatorial H atom.

The data in Table 3 indicate that CyOOH-initiation enhancement by concerted αH abstraction from CyOH faces a barrier that is 3.2 kcal mol^{-1} lower than that of the analogous Q=O reaction; accordingly, the TST-evaluated k_{enh}^{CyOH} of $\approx 6\times10^{-4}$ M^{-1} s^{-1}, is an order of magnitude higher than $k_{enh}^{Q=O}$. However, this sharp enhancement of CyOOH initiation by CyOH is effectively countered by strong negative feedback effects. Firstly, the Q$^•$OH radicals resulting from both the CyOOH + CyOH reaction and the fast CyOH + CyOO$^•$ propagation reaction (Scheme 1c) will rapidly add O_2 to form Q(OH)OO$^•$, which immediately decomposes to Q=O + $HO_2^•$.[13] The $HO_2^•$ radicals are known to undergo very fast termination with CyOO$^•$ radicals, the diffusion-controlled rate constant being $\approx 2.0\times10^{9}$ M^{-1} s^{-1},[25] which is 500 times faster than that of the mutual CyOO$^•$ termination, as described above. In addition, the fast equilibrium $HO_2^• + ROOH \rightleftarrows H_2O_2 + ROO^•$ (barrier = 4.3 kcal mol^{-1} for R = CH_3) should convert a sizeable fraction of ROOH into the much less efficient chain initiator H_2O_2 (BDE of HO–OH and RO–OH is 50 and 40 kcal mol^{-1}, respectively), in agreement with our observations in CyOH-addition experiments, for CyH conversions below 1 %. A detailed quasi-steady state (QSS) analysis[30] confirms that the expected almost 50-fold increase of the initial initiation rate by addition of 1 mol % CyOH is almost entirely off-set by the negative feedback through $HO_2^•$. Indeed, the QSS-calculated concentration of the CyOO$^•$ chain propagator, which governs CyH consumption, was found to increase by only 20 %. This result is fully consistent with our experimental findings at 145 °C because 1) at a conversion of 0.5 % the CyOOH concentration equals 35 mM in the pure CyH autoxidation, versus 25 mM when 1 mol % CyOH is initially added and 2) the CyH oxidation rates—governed by [CyOO$^•$]—are nearly equal for these two cases.

The experimental ratio $k_{enh}^{Q=O}/k_{enh}^{CyOOH} = 17$, determined above, seems to be in contradiction with the computed barriers (Table 3). However, we need to take into account the more rigid character of the TS for the CyOOH + CyOOH initiation reaction, which owes its 3 kcal mol^{-1} lower barrier to internal hydrogen bonds that preclude the internal rotations i and ii in the TS of CyOOH + Q=O. The HOA-TST calculated ratio $k_{enh}^{Q=O}/k_{enh}^{CyOOH}$ of 2, including tunnelling corrections, is an underestimate, as the TS of CyOOH + Q=O features more internal rotation modes (vide supra). Moreover, the unstable $^•Cy_{-\alpha H}OOH$ product of the CyOOH + CyOOH → $^•Cy_{-\alpha H}OOH$ + CyO$^•$ + H_2O reaction, immediately expels its $^•$OH,[12] in the general direction of the CyO$^•$ product, which should favour geminate CyO$^•$ + $^•$OH combination, and hence result in the molecular products, CyOOH + H_2O + Q=O.

Examining the abstraction of the *terminal* H from CyOO–H by the $^•$OH breaking away from another CyO–OH molecule, we located a TS for this process at 21.2 kcal mol^{-1}. However, its ν_{RC} frequency of 1640 cm^{-1} is significantly higher than for analogous reactions in Table 3, and is a fingerprint of a pure H or proton transfer without any contribution of relative O–O motion. Although the O–O distance (1.89 Å) is enlarged in the TS, but less so than in the TS of CyOOH + Q=O (2.04 Å), this suggests re-constitution of the O–O bond after the TS. Indeed, we suspect this TS to connect to the zwitterion pair [ROO$^-$][$^+H_2$OOR] as reaction products, driven by the high electron affinity of ROO$^•$ and the high proton affinity of ROOH, which together with the large Coulombic attraction make this zwitterion-pair formation exothermic by ≈10 kcal mol^{-1}. Hence, this is a much more favourable pathway than the endothermic hydrogen-abstraction-enhanced radical formation. Unfortunately, we were unable to perform a rigorous intrinsic reaction coordinate (IRC) analysis of this reaction as DFT fails to describe the long-range interactions involved in such an IRC analysis, and other high-level ab initio methods are beyond our computational resources for such large reaction systems.[35]

The newly proposed hydrogen-abstraction-assisted mechanism also readily explains the higher k_{enh} for butyric acid (soluble mimic of adipic acid) than for benzoic acid. The C–H bonds of the secondary α-hydrogens of butyric acid are weakened by a similar resonance-stabilization effect as for Q=O. Molecules, such as benzoic acid and 1-methyl-cyclohexanol, without weakened C–H bonds, are only efficiently active in the CyOOH-homolysis enhancement through the slower hydrogen-bond mechanism explained above.

CyOOH initiation revisited: Based on these new insights, one can question whether the "pure" CyOOH initiation in the liquid phase is indeed a unimolecular homolytic dissociation. As shown above, the efficiency of such a homolytic bond cleavage in the liquid phase is probably very small, if not negligible. We propose that even the so-called pure initiation reaction is actually enhanced by a concerted hydrogen abstraction from CyH. The barrier for reaction given in

Equation (25) is found to be only slightly higher than that of the Q=O-enhanced initiation reaction.

$$\mathrm{CyOOH + CyH \rightarrow CyO^{\bullet} \cdots HOH + Cy^{\bullet}} \qquad (25)$$

The TS is slightly "later", that is, more product-like (O···O distance of 2.11 Å), and the significantly lower ν_{RC} frequency of $1170\,\mathrm{cm^{-1}}$ shows a larger contribution of relative O−O motion. Moreover, given the C−H BDE in CyH of $\approx 96\,\mathrm{kcal\,mol^{-1}}$ (i.e., $9\,\mathrm{kcal\,mol^{-1}}$ more than the αC−H bond in Q=O), the reaction in Equation (25) is endothermic by $12.5\,\mathrm{kcal\,mol^{-1}}$, so that the potential energy drop after the TS is much smaller than in the Q=O enhanced reaction above (Figure 7). In addition, because the $\mathrm{Cy^{\bullet}}$ product radical is more reactive than the resonance-stabilized ketonyl radical and lacks the solvation screening that protects $\mathrm{^{\bullet}Q_{-\alpha H}{=}O}$, in-cage recombination of $\mathrm{Cy^{\bullet} + {}^{\bullet}OCy}$ is expected to be much more important. Based on the measured k_{diss} ($1.0\times10^{-6}\,\mathrm{s^{-1}}$), and given $[\mathrm{CyH}] = 9.3\,\mathrm{M}$, we calculate that the effective $k_{\mathrm{enh}}^{\mathrm{CyH}}$ should be only $\approx 1\times10^{-7}\,\mathrm{M^{-1}\,s^{-1}}$, which indicates that the majority of the nascent radicals indeed suffers "geminate" recombination. Thus, it appears that important in-cage radical recombination subsequent to the initiation step needs to be invoked to explain the rather low observed $k_{\mathrm{enh}}^{\mathrm{CyH}}/k_{\mathrm{enh}}^{\mathrm{Q=O}}$ ratio.

Arrhenius activation energies of the major initiation steps: The first-approximation method presented in above was used to measured the "pure" CyOOH initiation rate k_{diss} as well as $k_{\mathrm{enh}}^{\mathrm{Q=O}}$ at a temperature of 130 °C. This gave values of $5.0\times10^{-7}\,\mathrm{s^{-1}}$ and $7.3\times10^{-5}\,\mathrm{M^{-1}\,s^{-1}}$, respectively. Combination with the corresponding measurements at 145 °C yields Arrhenius activation energies of $25\pm5\,\mathrm{kcal\,mol^{-1}}$ for both. These results demonstrate clearly that even "pure" initiation in CyH autoxidation is not caused by unimolecular homolytic dissociation of CyO−OH, because this would require an activation energy close to $40\,\mathrm{kcal\,mol^{-1}}$. On the other hand, the experimental activation energies are fully consistent with the energy barriers computed for the bimolecular, hydrogen-abstraction-enhanced initiation processes identified in this work, thus corroborating the basic tenets of this work.

Conclusion

We have shown that radical-chain initiation in the main stage of cyclohexane autoxidation is largely caused by a concerted bimolecular reaction of the primary cyclohexyl hydroperoxide intermediate with cyclohexanone, a major oxygenated product. During this reaction, the breaking of the hydroperoxide O−O bond is assisted by simultaneous abstraction of a weakly bound αH atom from Q=O by the nascent $\mathrm{^{\bullet}OH}$ radical as it breaks away from the hydroperoxide. This process is argued to be highly efficient, as "geminate" in-cage recombination of the radical products $\mathrm{CyO^{\bullet}\cdots HOH}$ and $\mathrm{^{\bullet}Q_{-\alpha H}{=}O}$ is quasi-precluded by the combined effect of 1) dynamics-imposed translational separation of the two fragments, 2) screening of the $\mathrm{CyO^{\bullet}}$ radical site by the hydrogen-bonded $\mathrm{H_2O}$ molecule, 3) resonance-stabilization of the $\mathrm{^{\bullet}Q_{-\alpha H}{=}O}$ radical and 4) solvation shielding of the strongly polar $\mathrm{^{\bullet}Q_{-\alpha H}{=}O}$. In this way, Q=O greatly speeds up initiation and contributes significantly to the autocatalytic nature of the CyH autoxidation.

We also presented complementary theoretical and experimental evidence that so-called "pure" CyOOH initiation proceeds through a similar bimolecular process, involving concerted hydrogen abstraction from a CyH substrate molecule by the nascent $\mathrm{^{\bullet}OH}$. Although geminate $\mathrm{Cy^{\bullet}}$ and $\mathrm{CyO^{\bullet}}$ recombination is expected to be predominant for this case, it appears that the favourable energetics and the high concentration of the CyH reaction partner render this process much more efficient than the true unimolecular CyO−OH homolysis.

Acknowledgements

This work was performed as part of an IAP and a GOA project. I.H. is grateful to the FWO (Vlaanderen) for financial support and also thanks D. De Vos for useful comments.

[1] R. A. Sheldon, J.K. Kochi, *Metal-Catalyzed Oxidations of Organic compounds*, Academic Press, **1981**.

[2] C. A. Tolman, J. D. Druliner, M. J. Nappa, N. Herron, in *Activation and Functionalization of Alkanes* (Ed.: C. L. Hill), Wiley, **1989**, pp. 303.

[3] G. Franz, R. A. Sheldon, *Oxidation, Ullmann's Encyclopedia of Industrial Chemistry*, Wiley-VCH, **2000**.

[4] S. Bhaduri, D. Mukesh, *Homogeneous Catalysis, Mechanisms and Industrial Applications*, Wiley, **2000**.

[5] I. V. Berezin, E. T. Denisov, N. M. Emanuel, *The Oxidation of Cyclohexane*, Pergamon Press, **1966**.

[6] U. Schuchardt, D. Cardoso, R. Sercheli, R. Pereira, R. S. da Cruz, M. C. Guerreiro, D. Mandelli, E. V. Spinacé, E. L. Pires, *Appl. Catal. A* **2001**, *211*, 1.

[7] M. T. Musser, *Cyclohexanol and Cyclohexanone, Ullmann's Encyclopedia of Industrial Chemistry*, Wiley-VCH, **2000**.

[8] G. W. Burton, K. U. Ingold, *Acc. Chem. Res.* **1986**, *19*, 194.

[9] H.-D. Belitz, W. Grosch, *Food Chemistry*, Springer, Berlin, Heidelberg, **1999**.

[10] I. Hermans, T. L. Nguyen, P. A. Jacobs, J. Peeters, *ChemPhysChem* **2005**, *6*, 637 and Supporting Information.

[11] I. Hermans, P. A. Jacobs, J. Peeters, *J. Mol. Catal. A* **2006**, in press.

[12] L. Vereecken, T. L. Nguyen, I. Hermans, J. Peeters, *Chem. Phys. Lett.* **2004**, *393*, 432.

[13] I. Hermans, J.-F. Müller, T. L. Nguyen, P. A. Jacobs, J. Peeters, *J. Phys. Chem. A* **2005**, *109*, 4303.

[14] G. W. Parshall, S. D. Ittel, *Homogeneous Catalysis: the Applications and Chemistry of Catalysis by Soluble Transition Metal Complexes*, 2nd ed, Wiley, New York, **1992**.

[15] I. L. Arest-Yakubovich, F. A. Geberger, T. V. Khar'kova, L. E. Mitauer, G. Z. Lipkina, *Kinet. Catal.* **1989**, *30*, 959.

[16] Gaussian 03, Revision B.03, M. J. Frisch, G. W. Trucks, H. B. Schlegel, G. E. Scuseria, M. A. Robb, J. R. Cheeseman, J. A. Montgomery, Jr., T. Vreven, K. N. Kudin, J. C. Burant, J. M. Millam, S. S. Iyengar, J. Tomasi, V. Barone, B. Mennucci, M. Cossi, G. Scalmani, N. Rega, G. A. Petersson, H. Nakatsuji, M. Hada, M. Ehara, K. Toyota, R. Fukuda, J. Hasegawa, M. Ishida, T. Nakajima, Y. Honda, O. Kitao, H. Nakai, M. Klene, X. Li, J. E. Knox, H. P. Hratchian, J. B. Cross, V. Bakken, C. Adamo, J. Jaramillo, R. Gomperts, R. E. Stratmann, O. Yazyev, A. J. Austin, R. Cammi, C. Pomelli, J. W.

Ochterski, P. Y. Ayala, K. Morokuma, G. A. Voth, P. Salvador, J. J. Dannenberg, V. G. Zakrzewski, S. Dapprich, A. D. Daniels, M. C. Strain, O. Farkas, D. K. Malick, A. D. Rabuck, K. Raghavachari, J. B. Foresman, J. V. Ortiz, Q. Cui, A. G. Baboul, S. Clifford, J. Cioslowski, B. B. Stefanov, G. Liu, A. Liashenko, P. Piskorz, I. Komaromi, R. L. Martin, D. J. Fox, T. Keith, M. A. Al-Laham, C. Y. Peng, A. Nanayakkara, M. Challacombe, P. M. W. Gill, B. Johnson, W. Chen, M. W. Wong, C. Gonzalez, J. A. Pople, Gaussian, Inc., Wallingford CT, **2004**.

[17] a) A. D. Becke, *J. Chem. Phys.* **1992**, *96*, 2115; A. D. Becke, *J. Chem. Phys.* **1992**, *97*, 9173; A. D. Becke, *J. Chem. Phys.* **1993**, *98*, 5648; b) C. Lee, W. Yang, R. G. Parr, *Phys. Rev. B* **1988**, *37*, 785.

[18] A. M. Mebel, K. Morokuma, M. C. Lin, *J. Chem. Phys.* **1995**, *103*, 7414.

[19] H. Eyring, *J. Chem. Phys.* **1935**, *3*, 107.

[20] J. I. Steinfeld, J. S. Francisco, W. L. Hase, *Chemical Kinetics and Dynamics*, Prentice Hall, New Jersey, **1989**.

[21] a) L. Vereecken, J. Peeters, *J. Chem. Phys.* **2003**, *119*, 5159; b) L. Vereecken, J. Peeters, *J. Phys. Chem. A* **1999**, *103*, 1768.

[22] a) C. Eckart, *Phys. Rev.* **1930**, *35*, 1303; b) I. V. Tokmakov, J. Park, S. Gheyas, M. C. Lin, *J. Phys. Chem. A* **1999**, *103*, 3636.

[23] W. Forst, *Unimolecular Reactions*, Cambridge University Press, **2003**.

[24] The characteristic lifetime τ of CyOO$^•$ radicals is given by $1/\{[\mathrm{CyOO}^•]\,2k_{\mathrm{term}}\}$. At $\approx 0.1\,\%$ CyH conversion, [CyOO$^•$] is already as high as $\approx 5\times10^{-8}\,\mathrm{M}$ (derived experimentally from $\mathrm{d}\Sigma P/\mathrm{d}t/\{k^{\mathrm{CyH}}[\mathrm{CyH}]\}$), and hence τ as low as $\approx 2.5\,\mathrm{s}$, given $2k_{\mathrm{term}} = 8.4\times10^{6}\,\mathrm{M}^{-1}\mathrm{s}^{-1}$.[3] This CyOO$^•$ lifetime is much shorter than the timescale of $\approx 2000\,\mathrm{s}$ over which [CyOO$^•$] changes significantly, such that a [CyOO$^•$] quasi-steady state will be established immediately and maintained throughout the oxidation process.

[25] This value is based on the gas-phase rate constant for $\mathrm{HO_2}^• + \mathrm{ROO}^•$, in which R = C_6 alkyl, $k_{\mathrm{gas}} = 9.0\times10^{9}\,\mathrm{M}^{-1}\mathrm{s}^{-1}$ (A. A. Boyd, P. M. Flaud, N. Daugey, R. Lesclaux, *J. Phys. Chem. A* **2003**, *107*(6), 818), combined with the diffusion rate in the liquid phase $k_{\mathrm{diff}} = 2.7\times10^{9}\,\mathrm{M}^{-1}\mathrm{s}^{-1}$, assuming a diffusion coefficient of $10^{-5}\,\mathrm{cm^2 s^{-1}}$ in CyH and a reaction radius of 3.5 Å. The effective termination rate constant in the liquid phase can thus be estimated as $1/\{(1/k_{\mathrm{gas}})+(1/k_{\mathrm{diff}})\} = 2\times10^{9}\,\mathrm{M}^{-1}\mathrm{s}^{-1}$.

[26] $n_{\mathrm{O_2}}$ is the total amount of oxygen molecules present in the reactor; V_{liq} is the volume of the liquid phase in which O_2 is actually consumed. Because in our experiments $V_{\mathrm{liq}} = V_{\mathrm{gas}}$, and taking account of the Henry equilibrium between the gas phase and the liquid phase ($H = [\mathrm{O_2,gas}]/[\mathrm{O_2,liquid}] = 1104/T(\mathrm{K})$, A. K. Suresh, T. Sridhar, O. E. Potter, *AIChE J.* **1988**, *34*, 55), one can write for the O_2 consumption rate: $-\frac{1}{V_{\mathrm{liq}}}\frac{\mathrm{d}n_{\mathrm{O_2}}}{\mathrm{d}t} = \frac{1}{RT}\frac{\mathrm{d}p_{\mathrm{O_2}}}{\mathrm{d}t}(1+H(T))$.

[27] Equation (17) is derived by division of $-\frac{1}{V_{\mathrm{liq}}}\frac{\mathrm{d}n_{\mathrm{O_2}}}{\mathrm{d}t} = \{k^{\mathrm{CyH}}[\mathrm{CyH}] + k^{\mathrm{CyOOH}}[\mathrm{CyOOH}](t)\}[\mathrm{ROO}^•](t)$ by $\frac{\mathrm{d[CyOOH]}}{\mathrm{d}t} = \{p\,k^{\mathrm{CyH}}[\mathrm{CyH}] - s\,k^{\mathrm{CyOOH}}[\mathrm{CyOOH}](t)\}[\mathrm{ROO}^•](t)$.

[28] Equation (19) is the solution of the differential equation $\frac{\mathrm{d[CyOOH]}}{\mathrm{d}t} = \{p\,k^{\mathrm{CyH}}[\mathrm{CyH}] - s\,k^{\mathrm{CyOOH}}[\mathrm{CyOOH}](t)\}[\mathrm{ROO}^•](t)$ after substituting the QSS concentration of CyOO$^•$ radicals, Equation (10).

[29] I. Hermans, J. Peeters, P. A. Jacobs, *ChemPhysChem* **2006**, in press.

[30] See the Supporting Information.

[31] Owing to a vinoxy-type resonance and ring-strain reduction in the ketonyl radical; calculated at the B3LYP/6-311++G(df,pd)//B3LYP/6-31G(d,p)-level.

[32] L. Vereecken, J. Peeters, *Chem. Phys. Lett.* **2001**, *333*, 162.

[33] S. W. Benson, *The Foundations of Chemical Kinetics*, McGraw-Hill, New York, **1960**.

[34] E. Turpin, C. Fittschen, A. Tomas, P. Devolder, *J. Atmos. Chem.* **2003**, *46*, 1, and references therein

[35] a) D. C. Young, *Computational Chemistry*, Wiley, New York, **2001**; b) W. Koch, M. C. Holthausen, *A Chemist's Guide to Density Functional Theory*, 2nd ed., Wiley-VCH, **2001**.

Received: February 9, 2006